Electric field control of domain wall propagation in Pt/Co/GdOx films

Uwe Bauer, Satoru Emori, and Geoffrey S. D. Beach[a)]
Department of Materials Science and Engineering, Massachusetts Institute of Technology, Cambridge, Massachusetts 02139, USA

(Received 4 April 2012; accepted 23 April 2012; published online 9 May 2012)

The influence of a gate voltage on domain wall (DW) propagation is investigated in ultrathin Pt/Co/gadolinium oxide (GdOx) films with perpendicular magnetic anisotropy. The DW propagation field can be enhanced or retarded by an electric field at the Co/GdOx interface and scales linearly with gate voltage up to moderate bias levels. Higher gate voltage levels, corresponding to electric fields >0.2 V/nm, produce a large irreversible change to the magnetic anisotropy that can enable nonvolatile switching of the coercivity. © *2012 American Institute of Physics*. [http://dx.doi.org/10.1063/1.4712620]

Many proposed spintronic devices rely on domain wall (DW) dynamics to achieve logic and nonvolatile memory functionalities.[1–3] So far, control of DWs in such devices has relied on magnetic fields and current-induced spin transfer torques which are often associated with prohibitively high power consumption. The introduction of voltage gated effects would allow low power operation while adding an additional degree of freedom to enable further device capabilities. Voltage control of the magnetization is most often achieved using complex materials such as multiferroic oxides,[4] magnetic semiconductors,[5,6] or strain coupled magnetostrictive/piezoelectric composites.[7] However, direct electrical control of magnetic anisotropy[8–11] has recently been realized in metal ferromagnets at room temperature. This effect has been exploited to realize magnetization switching in magnetic tunnel junctions[12,13] and nonvolatile control of the magnetization vector in magnetoelectric charge trap memory cells.[14] Control of magnetic anisotropy should also allow for electric field control of DW dynamics,[15] which so far has received comparatively little attention.[16,17]

In this letter, we report direct electric field control of DW propagation in Pt/Co/gadolinium oxide (GdOx) films with perpendicular magnetic anisotropy (PMA). We show that DW propagation can be enhanced or retarded by an electric field applied at the Co/GdOx interface via modulation of the activation energy barrier that governs DW creep dynamics. By contrast, no clear influence on DW nucleation is observed due to the stochastic nature of nucleation events throughout the film. We further identify two regimes of electric field effects in the Co/GdOx system. In the low-field regime (<0.2 V/nm), the DW propagation field varies linearly and reversibly with the applied electric field. However, higher electric fields (0.2–0.4 V/nm) produce a large irreversible change to the magnetic anisotropy that enables nonvolatile switching of the coercivity of the Co film.

Films were prepared by dc magnetron sputtering at room temperature under 3 mTorr Ar with a background pressure of 1×10^{-7} Torr. A schematic of the sample structure is shown in Fig. 1(a). First, a continuous Ta(4 nm)/Pt(3 nm)/Co(1 nm)/GdOx(40 nm) film was deposited on a Si(100) substrate with a 50 nm thick thermally grown oxide layer. The GdOx layer was deposited by reactive sputtering from a metal Gd target at an oxygen partial pressure of $\sim 5 \times 10^{-5}$ Torr. After breaking vacuum, 100 μm diameter Ta(1 nm)/Au(5 nm) gate electrodes were deposited through a shadow mask. The metal gate was thick enough to provide good electrical contact but thin enough to allow optical access to the Co film.[18] Magnetic properties were probed via the polar magneto optical Kerr effect (MOKE), using a 532 nm diode laser attenuated to 1 mW, focused to a $\sim 5\,\mu$m diameter probe spot and positioned by a high resolution scanning stage. The switching field H_c and remnant to saturation magnetization ratio M_r/M_s were derived from hysteresis loops measured at a 17 Hz sweep rate. A mechanically compliant 15 μm diameter BeCu probe tip was used to apply a gate voltage V_g to the top electrode, while a 25 μm diameter blunt W microprobe was used to mechanically generate local DW nucleation sites as described below.

Pt/Co/M-oxide films (with $M =$ Al, Mg, etc.) are known to exhibit strong PMA originating in part from Co-O coordination at the Co/M-oxide interface.[19,20] Here, we have used GdOx as the gate oxide both because it has a high dielectric constant[21] and because of the expected contribution to spin-orbit coupling at the interface through the presence of a high-Z rare-earth ion. The as-deposited Pt/Co/GdOx films exhibit strong PMA with a hard axis (in-plane) saturation field of >5 kOe and square out-of-plane hysteresis loops (Fig. 1(b)). The switching field was stochastic, with H_c ranging from 240–280 Oe depending on the location on the film and at any given location varies by ± 10 Oe from cycle to cycle (Fig. 1(b)), which suggests magnetization reversal limited by random nucleation throughout the film.

When a W microprobe is landed with small mechanical overdrive on the GdOx surface in the vicinity of the MOKE spot (see Fig 1(a)), the hysteresis loops change markedly. As shown in Fig. 1(c), H_c drops to ~ 210 Oe at a distance of 50 μm from the location of the W tip, while the switching field distribution is greatly reduced. Moreover, H_c increases monotonically as a function of distance d from the W microprobe tip as shown in Fig. 1(d), indicating expansion of a circular domain centered at the contact point as the field is swept. This behavior can be explained by the creation of a local nucleation site with a reduced nucleation threshold

a)Author to whom correspondence should be addressed. Electronic mail: gbeach@mit.edu.

 © 2012 American Institute of Physics

Downloaded 15 May 2012 to 18.111.16.40. Redistribution subject to AIP license or copyright; see http://apl.aip.org/about/rights_and_permissions

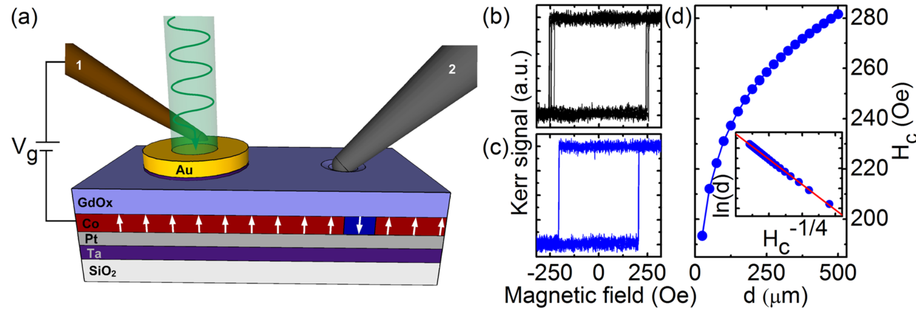

FIG. 1. (a) Schematic illustration of experimental setup including gated Pt/Co/GdOx structure, focused laser beam to measure polar MOKE hysteresis loops, BeCu microprobe (1) to apply gate voltage V_g, and W microprobe (2) to create local DW nucleation site to switch between DW nucleation and DW propagation limited magnetization reversal. White arrows illustrate local orientation of magnetization vector and DW nucleation beneath W probe tip. (b) Superposition of 6 individual MOKE hysteresis loops without landing W microprobe and (c) with W microprobe landed. (d) Switching field H_c as a function of distance between MOKE probing spot and tip of landed W microprobe. Inset of (d) shows same data but with ln(d) plotted as function of $H_c^{-1/4}$.

upon application of a local mechanical stress. In this case, H_c is determined by the propagation field required to drive domain expansion via DW motion. The narrow spread in H_c from cycle to cycle after creating the local nucleation site is consistent with DW creep through a fine scale disorder potential. In Fig. 1(d), inset, we show that H_c and d are related via a scaling relation $\ln(d) \sim H_c^{-1/4}$, which is identical to the scaling relation between DW velocity and applied field in the two-dimensional creep regime.[22] The distance d and the average DW velocity $\bar{v}$ during domain expansion are related by $d = \bar{v}\,\tau$, where τ is a time constant related to the field sweep rate. Thus, the observed scaling supports the identification of H_c as the DW propagation field.

We find that if the W microprobe overdrive is not too great, the sample returns to its original higher H_c state when the microprobe is lifted and the stress is relieved, which shows that no permanent damage arises from landing the W probe. This simple technique thereby provides a means to separately examine nucleation-limited and propagation-limited DW dynamics and the influence of a gate voltage on these processes.

In order to measure the voltage dependence of H_c in the nucleation and propagation-limited cases, we have used a second microprobe to apply a gate voltage to the Au gate electrode (Fig. 1(a)). This second probe tip was a more mechanically compliant BeCu probe, which could be brought into electrical contact with the Au electrodes without causing any changes to the measured hysteresis loops. Figure 2 shows H_c measured at the center of a Au gate electrode as a gate voltage V_g was cycled from +7.5 V to −7.5 V before (Fig. 2(a)) and after (Fig. 2(b)) landing a W probe ~80 μm away from the Au gate. Hysteresis loops were measured after every 0.5 V step by averaging 50 reversal cycles to account for stochasticity in the nucleation-limited case. In the DW nucleation limited regime, i.e., without landing the W microprobe, we observe a random fluctuation of H_c of about 8 Oe throughout the measurements despite signal averaging, but with no clear correspondence to the applied gate voltage (see Fig. 2(a)). The lack of a clear correlation between H_c and V_g suggests that the distribution of random nucleation events throughout the Co film rather than within the area covered by the gate electrode dominates magnetization reversal.

When a local nucleation site is created by the W microprobe close to the gate electrode, a clear modulation of H_c by V_g becomes apparent (Fig. 2(b)). In this case, H_c tracks V_g linearly and reversibly over a range of ~8 Oe, corresponding to a slope of ~0.5 Oe/V. Negative V_g reduces H_c and therefore enhances DW propagation whereas positive V_g increases H_c and therefore retards DW propagation in the Co film. As DW propagation occurs by creep dynamics, the DW velocity v can be expressed by an Arrhenius relation, $v \sim \exp(-E_a/kT)$, where k is the Boltzmann constant, T the temperature, and E_a the activation energy for DW propagation. Moreover, $E_a \sim (H_{crit}/H)^{1/4}$ where H is the applied magnetic field and H_{crit} is a characteristic depinning field that

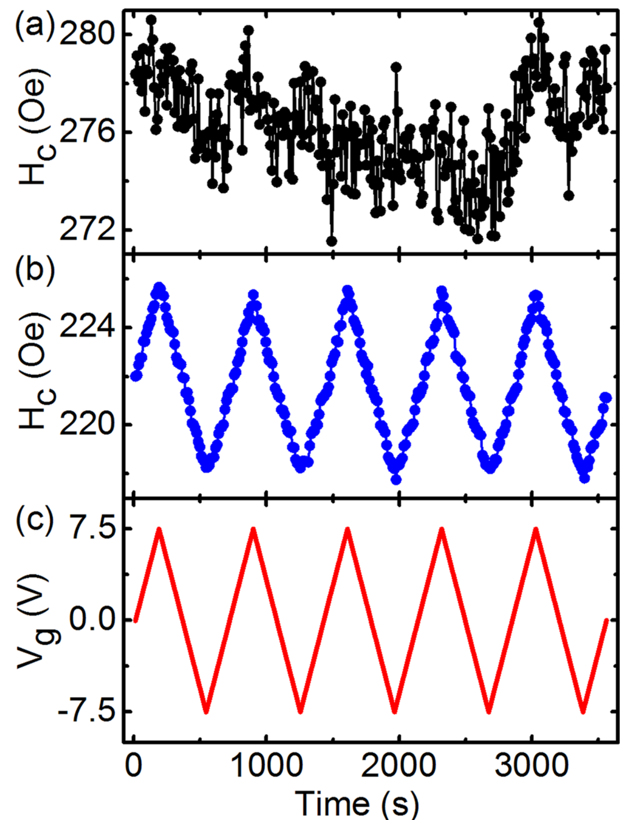

FIG. 2. Switching field H_c in (a) DW nucleation and (b) DW propagation limited regime (i.e., W microprobe landed at $d \sim 80\,\mu$m) and (c) gate voltage V_g plotted as a function of time. V_g is ramped between −7.5 V and +7.5 V for 5 cycles and 50 MOKE hysteresis loops are averaged after every 0.5 V step in V_g.

Downloaded 15 May 2012 to 18.111.16.40. Redistribution subject to AIP license or copyright; see http://apl.aip.org/about/rights_and_permissions

scales with the DW elastic energy density $\varepsilon_{el} \sim (AK_u)^{1/2}$.[22] Here, A is the exchange constant and K_u is the uniaxial anisotropy constant. Since E_a scales with K_u, modulation of K_u by an electric field at the Co/GdOx interface correspondingly changes the DW creep velocity.

Voltage-induced changes to H_c are reversible as long as $|V_g| < 8$ V (electric field < 0.2 V/nm), which indicates that no significant charge trapping occurs in the GdOx layer or at the Co/GdOx interface.[14,23] At higher V_g, irreversibility appears in the H_c versus V_g response, with the change in H_c depending on V_g and the voltage dwell time. Figure 3 shows H_c (Fig. 3(a)), M_r/M_s (Fig. 3(b)), and the leakage current I_L (Fig. 3(c)) measured as V_g was ramped to increasing positive and increasing negative voltage for two separate electrodes, respectively, beginning from the virgin state. For positive V_g up to 8 V, we find that H_c increases linearly with V_g, with $M_r/M_s = 1$ and $I_L < 100$ pA. Between +8 and +15 V, H_c starts to deviate from its linear dependence on V_g and after an initially slow decrease, H_c drops dramatically by ~120 Oe or ~60% above +12 V. At the same time, M_r/M_s decreases significantly from 1 to 0.2 and I_L increases up to 40 nA. Above $V_g = +15$ V, we observe hard breakdown of the GdOx dielectric as can be seen from the jump in I_L to the externally set current limit of 0.5 μA.[24] After dielectric breakdown, H_c and M_r/M_s remain at their diminished values and no significant change is observed within hours after the breakdown occurred. Under negative V_g the devices show markedly different behavior, with no significant deviation from the linear dependence of H_c on V_g until dielectric breakdown occurs at $V_g = -11$ V. Also, no change in M_r/M_s is observed under negative V_g.

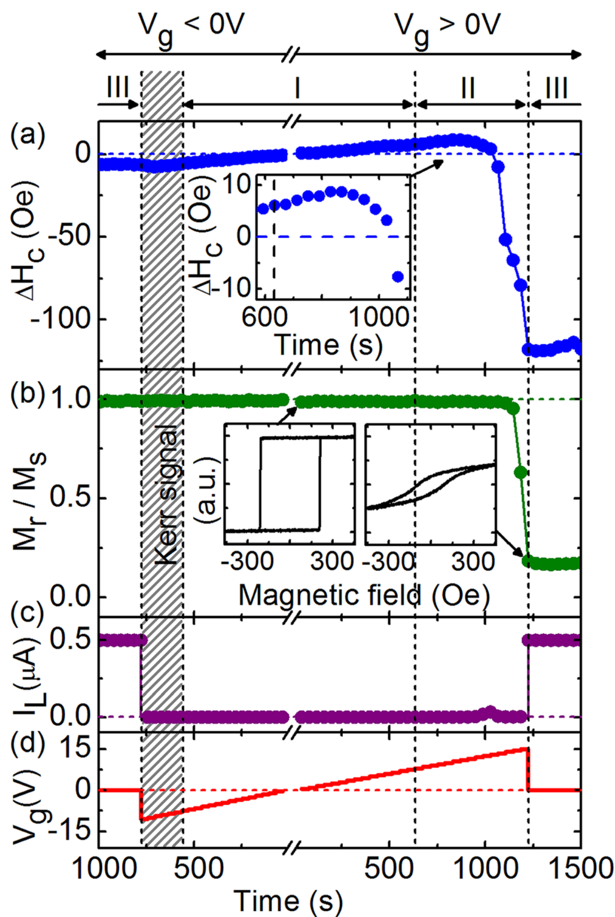

FIG. 3. (a) Modification of switching field H_c (i.e., ΔH_c), (b) remnant to saturation magnetization ratio M_r/M_s, and (c) leakage current I_L (clamped at 0.5 μA) as a function of time while gate voltage V_g is ramped in steps of 0.5 V every ~40 s (d). Left and right half of figure correspond to two different devices, measured under increasing negative and positive Vg, respectively. W microprobe is landed at $d \sim 80\,\mu$m and 250 MOKE hysteresis loops are averaged and I_L is measured after every voltage step. Effects in regime I are linear and reversible. Regime II (enlarged in inset of (a)) is marked by the onset of irreversibility and, at higher V_g, a steep drop in H_c and M_r/M_s. Regime III corresponds to hard dielectric breakdown. Dashed area highlights lack of regime II for negative V_g. Insets in (b) show representative hysteresis loops at indicated points.

From these observations, we separate the electric field effects into 3 regimes. In regime I, between $V_g = -8$ V to +8 V, DW propagation can be reversibly controlled by an electric field at the Co/GdOx interface, and H_c follows V_g linearly. In regime II, ($V_g = +8$ V to +15 V), H_c and M_r/M_s decrease significantly and irreversibly. In Regime III, corresponding to $V_g < -11$ V and $V_g > +15$ V, hard dielectric breakdown of the GdOx layer occurs, and no further changes in hysteresis characteristics are induced.

Since the strongest modifications of H_c and M_r/M_s in regime II occur at V_g close to regime III, it is likely that their origin is related to processes occurring during or directly preceding hard dielectric breakdown. Hard dielectric breakdown is typically preceded by a soft breakdown which is associated with trapped charge generation in the dielectric layer.[24] Trapped charges have previously been shown to result in strong modifications of magnetic anisotropy in ultrathin Fe films and could therefore explain the irreversible character of the modifications of H_c and M_r/M_s, observed here.[14] However, changes in O^{2-} coordination at the Co/GdOx interface could also play an important role in the observed effects.[24] Oxygen vacancy V_O^{2+} generation is often a precursor of dielectric breakdown in high-k gate oxides[25] and V_O^{2+} would migrate predominantly to the Co/GdOx interface due to the high positive V_g. Since hybridization between Co 3d and O 2p orbitals is expected to play a crucial role in the PMA of the Co film,[19,20,26] the PMA should be very sensitive to changes in interface oxygen stoichiometry.[19,20,27] Accumulation of oxygen vacancies at the interface could therefore significantly contribute to the observed loss of PMA in regime II. Moreover, hysteresis loops are only sensitive to changes at the interface between GdOx and the Co film but

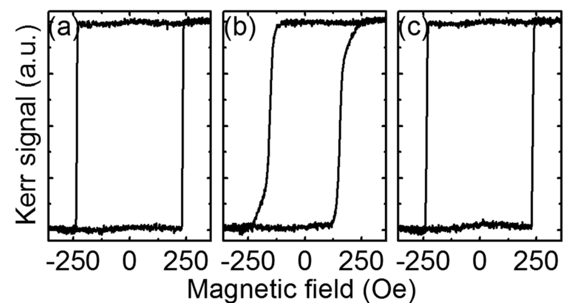

FIG. 4. Evolution of MOKE hysteresis loops measured for Pt/Co/GdOx/Ta/Au structure with reduced GdOx thickness of 3 nm. (a) Before application of gate voltage V_g, (b) after application of $V_g = +1.8$ V for 60 s, and (c) after subsequent application of $V_g = -1$ V for 15 s.

Downloaded 15 May 2012 to 18.111.16.40. Redistribution subject to AIP license or copyright; see http://apl.aip.org/about/rights_and_permissions

not to changes at the interface between GdOx and the gate electrode, which could explain why regime II is only observed at positive V_g.

Interestingly, the dramatic changes in H_c and M_r/M_s observed for positive V_g in Region II can be partially or even fully reversed by application of a negative V_g so long as hard breakdown has not been reached. In addition, the timescale and voltage levels necessary for these changes can be significantly reduced by reducing the GdOx thickness. Figure 4 shows a series of hysteresis loops measured for a Pt/Co/GdOx device with 3 nm thick GdOx. The (propagation-limited) H_c is 235 Oe before application of a gate voltage (Fig. 4(a)). $V_g = +1.8$ V was then applied for 60 s and then set to zero, after which H_c decreased to 160 Oe (Fig. 4(b)). This nonvolatile change in coercivity was retained until a negative gate voltage of -1 V was applied for 15 s, after which the coercivity returned to its initial state (Fig. 4(c)). It has been shown previously that the charge trapping and vacancy migration that occurs during soft breakdown of a dielectric can be reversed under appropriate conditions.[28,29] This behavior might therefore be exploited as a nonvolatile mechanism for switching the magnetic state electrically.

In summary, we have demonstrated direct electric field control of DW propagation in ultrathin Co films with perpendicular magnetic anisotropy. We find that the DW propagation field linearly follows the applied gate voltage and can be enhanced and retarded by the presence of an electric field at the Co/GdOx interface. Moreover, we identify two different regimes of electric field effects in the Co film. The low field regime allows reversible control of DW propagation whereas the high field regime allows nonvolatile control of magnetic anisotropy. We believe that these findings provide an important step towards the realization of ultralow power, voltage gated spintronic logic and memory devices.

This work was supported under NSF-ECCS-1128439. S.E. acknowledges financial support by the NSF Graduate Research Fellowship Program. Technical support from David Bono and Mike Tarkanian is gratefully acknowledged.

[1]D. A. Allwood, G. Xiong, C. C. Faulkner, D. Atkinson, D. Petit, and R. P. Cowburn, Science **309**, 1688 (2005).
[2]C. Chappert, A. Fert, and F. N. Van Dau, Nat. Mater. **6**, 813 (2007).
[3]S. S. P. Parkin, M. Hayashi, and L. Thomas, Science **320**, 190 (2008).
[4]R. Ramesh and N. A. Spaldin, Nat. Mater. **6**, 21 (2007).
[5]H. Ohno, D. Chiba, F. Matsukura, T. Omiya, E. Abe, T. Dietl, Y. Ohno, and K. Ohtani, Nature **408**, 944 (2000).
[6]D. Chiba, M. Yamanouchi, F. Matsukura, and H. Ohno, Science **301**, 943 (2003).
[7]W. Eerenstein, N. D. Mathur, and J. F. Scott, Nature **442**, 759 (2006).
[8]M. Weisheit, S. Fahler, A. Marty, Y. Souche, C. Poinsignon, and D. Givord, Science **315**, 349 (2007).
[9]T. Maruyama, Y. Shiota, T. Nozaki, K. Ohta, N. Toda, M. Mizuguchi, A. A. Tulapurkar, T. Shinjo, M. Shiraishi, S. Mizukami, Y. Ando, and Y. Suzuki, Nat. Nanotechnol. **4**, 158 (2009).
[10]M. Endo, S. Kanai, S. Ikeda, F. Matsukura, and H. Ohno, Appl. Phys. Lett. **96**, 212503 (2010).
[11]A. Mardana, S. Ducharme, and S. Adenwalla, Nano Lett. **11**, 3862 (2011).
[12]Y. Shiota, T. Nozaki, F. Bonell, S. Murakami, T. Shinjo, and Y. Suzuki, Nat. Mater. **11**, 39 (2012).
[13]W. G. Wang, M. G. Li, S. Hageman, and C. L. Chien, Nat. Mater. **11**, 64 (2012).
[14]U. Bauer, M. Przybylski, J. Kirschner, and G. S. D. Beach, Nano Lett. **12**, 1437 (2012).
[15]S. Emori and G. S. D. Beach, Appl. Phys. Lett. **98**, 132508 (2011).
[16]T. K. Chung, G. P. Carman, and K. P. Mohanchandra, Appl. Phys. Lett. **92**, 112509 (2008).
[17]T. H. E. Lahtinen, J. O. Tuomi, and S. van Dijken, Adv. Mater. **23**, 3187 (2011).
[18]Z. Q. Qiu and S. D. Bader, J. Magn. Magn. Mater. **200**, 664 (1999).
[19]A. Manchon, S. Pizzini, J. Vogel, V. Uhlir, L. Lombard, C. Ducruet, S. Auffret, B. Rodmacq, B. Dieny, M. Hochstrasser, and G. Panaccione, J. Appl. Phys. **103**, 07A912 (2008).
[20]B. Rodmacq, A. Manchon, C. Ducruet, S. Auffret, and B. Dieny, Phys. Rev. B **79**, 024423 (2009).
[21]T. M. Pan, C. S. Liao, H. H. Hsu, C. L. Chen, J. D. Lee, K. T. Wang, and J. C. Wang, Appl. Phys. Lett. **87**, 262908 (2005).
[22]S. Lemerle, J. Ferre, C. Chappert, V. Mathet, T. Giamarchi, and P. Le Doussal, Phys. Rev. Lett. **80**, 849 (1998).
[23]F. Bonell, S. Murakami, Y. Shiota, T. Nozaki, T. Shinjo, and Y. Suzuki, Appl. Phys. Lett. **98**, 232510 (2011).
[24]S. Lombardo, J. H. Stathis, B. P. Linder, K. L. Pey, F. Palumbo, and C. H. Tung, J. Appl. Phys. **98**, 121301 (2005).
[25]K. L. Pey, N. Raghavan, X. Wu, W. H. Liu, X. Li, M. Bosman, K. Shubhakar, Z. Z. Lwin, Y. N. Chen, H. L. Qin, and T. Kauerauf, Microelectron. Eng. **88**, 1365 (2011).
[26]E. Y. Tsymbal and K. D. Belashchenko, J. Appl. Phys. **97**, 10C910 (2005).
[27]M. K. Niranjan, C. G. Duan, S. S. Jaswal, and E. Y. Tsymbal, Appl. Phys. Lett. **96**, 222504 (2010).
[28]R. Waser and M. Aono, Nat. Mater. **6**, 833 (2007).
[29]D. H. Kwon, K. M. Kim, J. H. Jang, J. M. Jeon, M. H. Lee, G. H. Kim, X. S. Li, G. S. Park, B. Lee, S. Han, M. Kim, and C. S. Hwang, Nat. Nanotechnol. **5**, 148 (2010).

Downloaded 15 May 2012 to 18.111.16.40. Redistribution subject to AIP license or copyright; see http://apl.aip.org/about/rights_and_permissions